Feed Distribution in Distillation: Assessing Benefits and Limits with Column Profile Maps and Rigorous Process Simulation

Daniel Beneke, Diane Hildebrandt, and David Glasser
Centre of Material and Process Synthesis (COMPS), Dept. of Chemical and Metallurgical Engineering, University of the Witwatersrand, Johannesburg, Gauteng, South Africa

DOI 10.1002/aic.13940
Published online November 7, 2012 in Wiley Online Library (wileyonlinelibrary.com).

This contribution describes the column profile map (CPM) methodology for designing distributed feed distillation columns. For non-sharp product distributions, a case study shows that energy savings of approximately 35% can be obtained if the feed stage(s) are designed optimally. Feed distribution allows capital cost savings, expands operating leaves, and can obtain greater separation feasibility. However, this column only has benefits in ternary and higer-order systems and when product distributions are non-sharp. To validate these counter-intuitive claims, a real Benzene, p-Xylene, Toluene system is modeled using CPMs, and the resulting design parameters are transported to Aspen Plus®. Using a sum of squared errors objective function to quantify savings, a cost saving trend very similar to the one predicted by the CPM method is obtained. This article therefore describes a complete design methodology for distributed feed systems and provides convincing evidence of benefits of such a system. © 2012 American Institute of Chemical Engineers *AIChE J,* 59: 1668–1683, 2013
Keywords: optimization, design (process simulation), distillation, energy, mathematical modeling

Introduction

The large scale separation of chemicals is an integral part of modern processing industries, used to produce final, high purity products or to improve the operation of downstream process units. Unfortunately, the separation step of a typical processing plant contributes significantly to the overall cost of the plant, which translates directly into the energy requirement of the process. It has been estimated that the cost of a separation structure on a typical plant accounts for around 50–80% of the overall plant operating costs.[1] Distillation has been, and probably will be for some time to come, the most utilized means of separation because it has good economic properties at large scale and the design and operation procedure is reasonably well understood. However, due to the rising costs of energy, researchers and design engineers alike have been forced to critically relook the energy efficiency of distillation.

The minimum energy and equilibrium stage requirements of the classic single-feed-two-product distillation column (so-called simple columns) is quite well understood through techniques like the McCabe-Thiele method for binary systems.[2] The multicomponent simple column design problem is equally well known through techniques like the Fenske–Underwood–Gilliland equations, although this method is reliable only for near ideal and non-azeotropic systems. The boundary value method pioneered by Doherty and coworkers can take into account non-ideal phase equilibrium behaviour, and approximates the compositional change in a distillation column though a set of differential equations.[3–5] This method allows one to easily infer minimum energy demands (directly proportional to column reflux), the stage requirement of the column as well as the feed stage position. Moreover, this method has been validated with rigorous process simulation software.[6] Another, more recent approach using the shortest stripping line[7] has been shown to find column sequences that contain non-pinched, minimum energy columns within a sequence as well as accounting for heat integration and capital/operational cost trade-offs, using numerical optimization techniques.[8]

Although simple columns represent the most fundamental piece of distillation equipment, and are probably the most well understood through the development of the aforementioned techniques, it is thought that there are larger energy savings in so-called complex columns, that is, column structures with more than one feed and/or two products. One such example, the Petlyuk column, has received substantial attention in the literature,[9–17] with typical savings of around 30% of energy costs being reported.[12]

Although the distillation design problem seems to be well studied, one can not help but wonder whether there are advantageous structures that have not been considered yet, or that have been missed or discarded by current design techniques. Recently, a column profile map (CPM) technique was proposed as a graphical means of designing columns.[18,19] The method is an adaption of the differential equations developed by Doherty et al., but importantly, the CPM method and its governing equations are universal, meaning that the design of even the most complex column is a relatively straightforward extension from simple column design. In fact, complex columns are almost encouraged through this method because it has been shown that useful

Correspondence concerning this article should be addressed to D. Beneke at Daniel.Beneke@sasol.com.

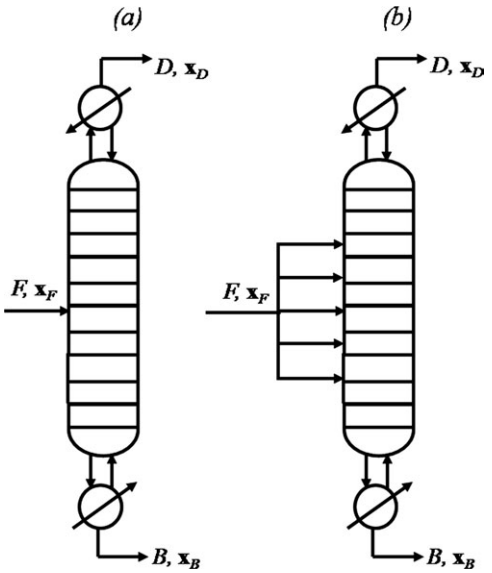

Figure 1. Representation of a (a) simple column, and (b) distributed feed column.

mathematical and topological phenomena arise through the operating conditions of complex columns.[17,20,21]

Now, the easiest means of "creating" a complex column is by merely choosing not to add all the feed to the column at one particular location, but to distribute the feed along the length of the column, as shown in Figure 1b. At first glance this may seem useless, and in many cases, it may very well be. This problem has been partially tackled by other researchers through the Underwood equations[22] and the boundary value method,[23] while other works have attempted to optimize multiple feed columns where each feed stream has a different feed composition.[24,25] Although all of these previous works have successfully described the distributed feed problem mathematically, none of them have pointed out the advantages of doing so. In the authors' opinion, this is because other design techniques are not generalized (unlike the CPM method), and, therefore, extracting insights into complex columns are often difficult. In fact, it has been explicitly stated that distributed feed columns do not alter the basic operation of the column and only complicates analysis.[26]

In this artcle, it will be shown that the distributed feed column can hold significant advantages for ternary and higher order systems in terms of energy savings, stage requirements, and even making separations that were previously considered unviable, viable. A relatively simple design procedure for these columns using the CPM method is shown, and it is pointed why other techniques like the McCabe-Thiele and Underwood methods may have missed this unique opportunity. It should be mentioned that this article builds on ideas first put forward by Holland[27] in his PhD thesis, also using a CPM approach.

This article is outlined as follows: The "CPMs" Section gives an overview of the CPM technique, opportunities available in complex columns, and simple column design. The "Distributed Feed Columns" Section addresses the design of distributed feed columns, while the "Benefits of Distributing the Feed" and "Limitations" Sections highlight the benefits and limitations of this type of column, respectively. The "Validation with Aspen Plus" Section convincingly illustrates how the CPM designs for distributed feed columns give rise to excellent initialization values for Aspen Plus®, and shows that Aspen Plus® agrees reasonably well with CPM predictions. Finally, the "Discussion and Conclusions" Section gives an account of the major findings and results of the work.

CPMs

Background

The fundamental building block in the CPM design methodology is the generalized column section (CS), depicted in Figure 2. By definition, a CS is a length of column between points of material or energy influx or efflux. This CS allows one to piece together any column structure, regardless of its complexity. For example, the simple column shown in Figure 1a will consist of two CSs, above and below the feed, while the distributed feed column consists of many CSs, depending on how many times the feed is distributed.

Using the stream definitions in Figure 2, it is possible to derive a first order differential equation using a Taylor expansion, as shown in Eq. 1.

$$\frac{d\mathbf{x}}{dn} = \left(1 + \frac{1}{R_\Delta}\right)(\mathbf{x} - \mathbf{y}) + \left(\frac{1}{R_\Delta}\right)(\mathbf{X}_\Delta - \mathbf{x}) \tag{1}$$

where

$$R_\Delta = \frac{L}{V - L} = \frac{L}{\Delta} \quad \text{and} \quad \mathbf{X}_\Delta = \frac{V\mathbf{y}^T - L\mathbf{x}^T}{\Delta} = \frac{V\mathbf{y}_{n+1} - L\mathbf{x}_n}{\Delta}$$

Equation 1 is known as the difference point equation (DPE) and describes the change in liquid composition ($\mathbf{x}$) in a CS as the stage number (n) progresses. The vapour composition ($\mathbf{y}$) is in equilibrium with the liquid composition on stage n and this relationship may be modeled with an appropriate phase equilibrium model. The superscript T denotes the top of the CS at stage number 0. This is merely a reference point and one may equivalently specify the bottom of the CS to be at stage 0. The R_Δ parameter is a generalized reflux dictating the ratio of liquid flowrate to the net flowrate. R_Δ may either be positive ($V > L$) as found in rectifying CSs, or negative when the CS is in stripping mode ($V < L$). Interestingly, when $R_\Delta = \infty$, the DPE is mathematically equivalent to the classic residue curve equation, from which a residue curve map may be constructed.[28–30] Residue curve maps have proven to be useful for distillation design because they summarize the phase equilibrium behaviour conveniently in one diagram. These maps can be constructed by integrating the DPE at infinite reflux conditions and selecting a range of coordinates from which to

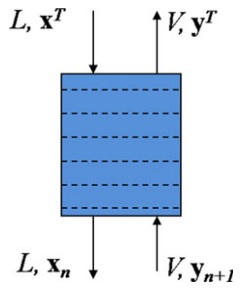

Figure 2. A generalized CS.

[Color figure can be viewed in the online issue, which is available at wileyonlinelibrary.com.]

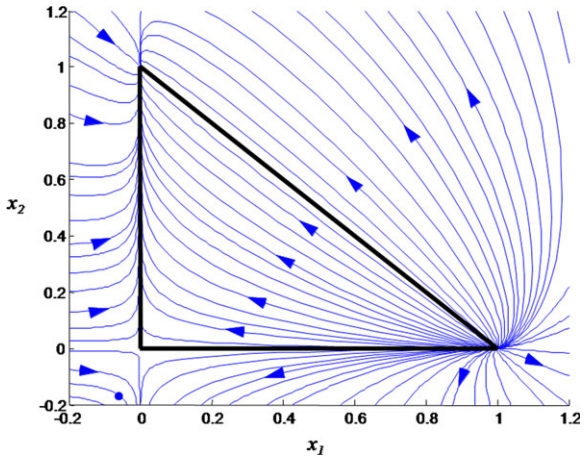

Figure 3. A residue curve map with α = [5,1,2].

[Color figure can be viewed in the online issue, which is available at wileyonlinelibrary.com.]

integrate from. Note that integration can be performed in both negative and positive direction of n, which, in terms of a CS, merely tracks composition changes up and downwards from the initial integration coordinate, respectively. Such a residue curve map is shown in Figure 3 for a constant relative volatility system with volatilities of $\boldsymbol{\alpha} = [5,1,2]$, representing the [low, high, intermediate] boiling components, respectively. The constant relative volatility model is given in Eq. 2.

$$y_i = \frac{\alpha_i x_i}{\sum \alpha_i x_i} \tag{2}$$

It is interesting to note that the residue curve map in Figure 3 is not bound by positive compositions from a mathematical point of view, even though it is physically impossible to obtain these negative compositions, that is, compositions outside the so-called mass balance triangle where $x_i < 0$ or $x_i > 1$. The use of viewing negative compositions has been discussed in other works on CPMs,[18,19,21,31] but it will again become apparent in subsequent discussions why it is useful. It is important to define the stationary points here as the stable node, the point where all profiles terminate at (the pure high boiling component), the unstable node, the point where all profiles originate from (the pure low boiling component), and finally the saddle point, the point where profiles initially travel toward but then swerve away from (the pure intermediate boiling component).

The final parameter in the DPE, $\mathbf{X}_\Delta$, is a pseudo compositional variable dictating the net flow of individual components in a CS. $\mathbf{X}_\Delta$ behaves in much the same way as a real composition would, as its element entries sum to unity. However, it is perfectly legitimate for $\mathbf{X}_\Delta$ to have negative elements which merely implies that the particular component is travelling opposite to the net flow direction in the CS. Once a phase equilibrium model, R_Δ, and $\mathbf{X}_\Delta$ have been specified, it is possible to construct a CPM. Figure 4 shows a CPM for the same constant relative volatility system given in Figure 3.

It is fascinating to note that at finite reflux conditions, the CPM is simply a topological transform of the residue curve map. The general curvature of the residue curve map has been retained, but the stationary points have been shifted in composition space—even to negative composition space. Specifically, the stable node has been shifted into positive composition space while the other points have been shifted outward. Furthermore, the profiles running exactly between the stationary points are straight, resulting in a so-called transformed triangle (TT) represented by the red lines in Figure 3, although this property is unique to constant relative volatility systems only. Obviously, different choices of R_Δ and $\mathbf{X}_\Delta$ will result in a different movement of the TT which in turn may lead to some counter-intuitive separation possibilities. Other works have discussed, in some detail, the advantages from a topological perspective of creative $\mathbf{X}_\Delta$ placements,[20,32] particularly in negative composition space. However, using standard separation equipment like simple columns severely restricts possible choices of $\mathbf{X}_\Delta$ and R_Δ, as shown in the following section.

Simple Column Design

Before investigating the distributed feed problem in further detail, it is necessary to understand the concepts of simple column design. As mentioned, the CPM technique for simple columns is essentially equivalent to the boundary value method of Doherty et al. The aim of this design approach is to find an intersection of the liquid composition profiles of adjacent CSs for fixed feed and product specifications. It can be shown that when CSs are terminated by a reboiler and condenser, as is the case in both CSs in the simple column, that $\mathbf{X}_\Delta$ is equal to the product specification in that particular CS, and the net flow parameter's (Δ) magnitude is equal to the product flowrate in that particular CS. Furthermore, the CS above the feed stage is always in rectifying mode and the CS below the feed is always in stripping mode, and the reflux ratios in these CSs are related by a mass balance across the feed stage through Eq. 3, where the subscript R and S indicate rectifying and stripping CSs, respectively.

$$R_{\Delta S} = \frac{L_S}{\Delta_S} = \frac{R_{\Delta R}\Delta_R + Fq}{\Delta_R - F} \tag{3}$$

Using the boundary value method, that is, specifying the desired product purities *a priori*, a degree of freedom analysis of a ternary simple column indicates that that three

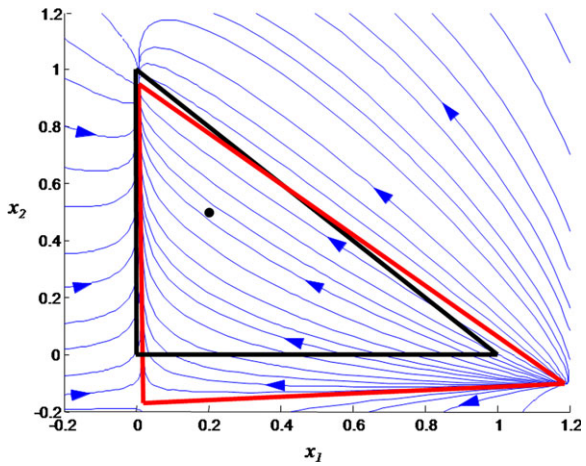

Figure 4. A CPM with R_Δ = 6, $\mathbf{X}_\Delta$ = [0.2,0.5] and α = [5,1,2].

[Color figure can be viewed in the online issue, which is available at wileyonlinelibrary.com.]

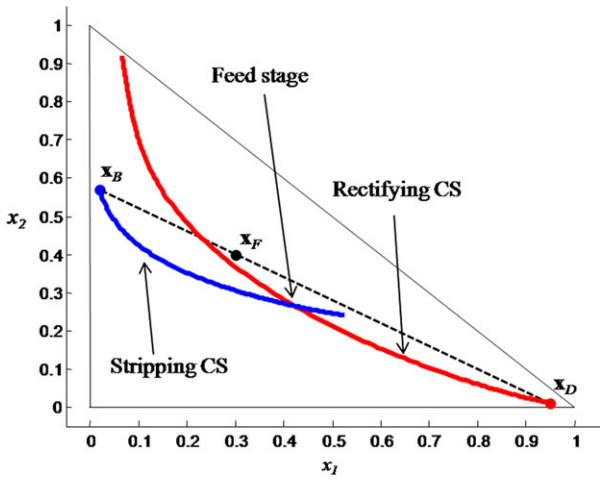

Figure 5. A feasible simple column design for the base case with $R_{\Delta R} = 3.5$.

[Color figure can be viewed in the online issue, which is available at wileyonlinelibrary.com.]

composition variables in the product streams be specified, assuming the feed is known. This means that all compositions in one product stream are completely specified and only one composition in the remaining product stream. Once this is known, all product flowrates may also be determined by mass balance. It should be noted that any three mass balance variables could have been specified in the products streams (product flows or compositions), it is just more convenient to specify compositions since these are the boundary conditions. All that remains in the design is to specify a reflux value for either CS which allows the DPE of both CSs to be fully specified (through Eq. 3), after which the corresponding profiles can be plotted. In both CSs, integration commences from the desired product specification in that CS at stage $n = 0$.

A feasible design is shown in Figure 5 for the $\boldsymbol{\alpha} = [5,1,2]$ system with $F = 1$ mol/s, $q = 1$, $\mathbf{x}_F = [0.3,0.4]$, $\mathbf{x}_D = [0.95,0.01]$, $\mathbf{x}_B = [0.02,0.57]$, $D = 0.301$ mol/s, $B = 0.699$ mol/s, $R_{\Delta R} = 3.5$, and $R_{\Delta S} = -2.94$. The product specifications used in this design will be used for all subsequent designs as a basis of comparison, and will be referred to as the base from this point onwards.

Figure 5 clearly demonstrates that the design is feasible since the liquid profiles intersect one another. By merely tracking the progression of the stage number as integration proceeds, it is simple to deduce the total number of equilibrium stages needed for the separation, as well as the location of the feed stage (the point of profile intersection). This specific design requires 11.6 stages and the feed stage is located on stage 5.3, assuming a total condenser and a partial reboiler is used and that the latter acts as an equilibrium stage. In this article, the point of profile intersection was determined through a minimum Euclidean distance criterion, as first shown by Zhang and Linninger.[6,33] The distance criterion was set at 0.005. For highly non-ideal ternary systems a design's feasibility can be assessed in approximately 5 s, while constant volatility systems can be assessed in less than 1 s. Furthermore, it can be seen that the profiles continue past one another by quite a large margin, meaning that the current operating conditions of the column are excessive. By reducing the reflux ratio until the stationary point of one of the profiles just falls on the other profile, the minimum reflux condition of the column has been reached and the column is said to have pinched. The minimum column reflux ($R_{\Delta R} = 2.07$) for the base case is shown in Figure 6. When a profile approaches a stationary point, the stage numbers tend toward infinity. Operating at minimum column reflux is thus an impractical operating condition but it serves as a basis of comparison for the minimum energy requirement between other structures.

Opportunities and limitations

From the preceding simple column designs, it is easy to see why the designer is so limited. The $\mathbf{X}_\Delta$ placements are specified beforehand through the product specifications and only a certain range of R_Δ values are permitted which will yield a feasible design. An interesting example of the dramatic effects that can be achieved through creative $\mathbf{X}_\Delta$ and R_Δ values, not attainable in simple columns, is shown in Figures 7a, b for the highly non-ideal Acetone/Methanol/Chloroform system, modeled using the NRTL activity coefficient model.

Figure 7a shows that the residue curve map contains four azeotropes (three binary and one ternary), indicated by red dots, implying that many separations will be difficult or impossible in this system. However, in the accompanying CPM in Figure 7b, profiles have been transformed to such an extent that all stationary points have been moved to negative composition space, resulting in many new separation possibilities. CSs operating under these specifications are however only possible in complex columns. Although non-ideal systems are not discussed further in this article, cases such as those in Figures 7a, b serve as a motivation for investigating complex structures, such as distributed feed columns, which allow some freedom in specifying variables to achieve effects like this.

Distributed Feed Columns

Structure and CS breakdown

A generic distributed feed column with its accompanying CS breakdown is shown in Figure 8. It can be seen that a feed divided into $N-1$ substreams will result in an overall column with N total CSs. For the sake of consistency, we

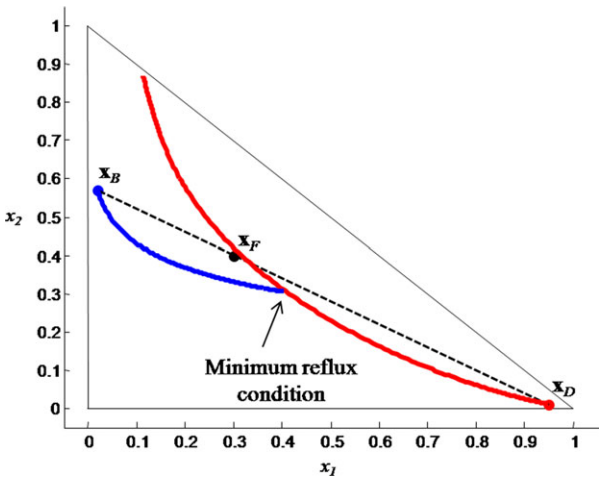

Figure 6. A minimum reflux design for the base case with $R_{\Delta R} = 2.07$.

[Color figure can be viewed in the online issue, which is available at wileyonlinelibrary.com.]

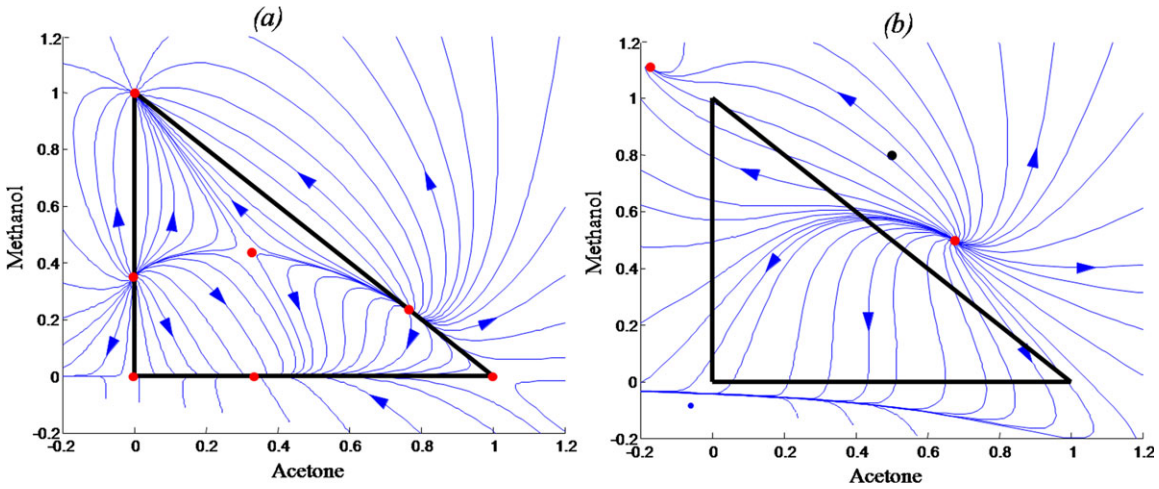

Figure 7. The Acetone/Methanol/Chloroform system at (a) residue curve map conditions and (b) CPM conditions with $R_\Delta = -3$ and $X_\Delta = [0.7,0.5]$.

[Color figure can be viewed in the online issue, which is available at wileyonlinelibrary.com.]

will still refer to the top and bottommost CSs as rectifying and stripping CSs, denoted by subscripts R and S, respectively. These two CSs are again the product producing CSs and behave in much the same way as the CSs in the simple column, that is, their $\mathbf{X}_\Delta$ values will be set by the product specifications of the column. It will also be assumed that the stripping CS is terminated by a total condenser while the rectifying CS is terminated by a partial reboiler, standard practice in distillation design.

Reflux ratio effects

According to the definition of the generalized reflux ratio in a CS, distributing the feed to different points throughout the column will change the generalised reflux ratio in each new CS. In determining the refluxes of CSs in the column, it is convenient to define a "reference" reflux from which to work. For this, we shall use the topmost CS to keep with convention of simple columns, although this choice is completely arbitrary. The value of this reflux is also referred to as the overall column reflux and this quantity is directly related to the energy requirement of the column. If we only consider for the moment two generic CSs located across a feed point between CS_{k-1} and CS_k, we can perform a mass balance, as shown in Figure 9.

We now have streams in CS_k written in terms of the stream of CS_{k-1}, which allows us to relate their refluxes (and net flows) using the definition of R_Δ in the DPE:

$$R_{\Delta k} = \frac{L_k}{\Delta_k} = \frac{R_{\Delta k-1}\Delta_{k-1} + F_{k-1}q_{k-1}}{\Delta_{k-1} - F_{k-1}} \tag{4}$$

As the reflux in the rectifying CS has been specified (the reference reflux), and the net flow in this CS is also known (product flowrate D), it is possible to determine the reflux ratio in CS_2 by knowing the magnitude and condition of the sub feed stream F_1. This procedure can be continued until the reflux ratios in all the CSs have been determined. From the top of the column downwards, each subsequent feed addition (assuming a pure liquid feed) has the effect of increasing the reflux, as the net flow quantity in the denominator becomes smaller. When enough feed material has been added, the CS switches to stripping mode as L becomes larger than V. Interestingly, for a certain value of the reference reflux in the rectifying CS, the reflux ratio in the stripping CS is exactly the same in the simple column as that in the distributed feed column, assuming the overall feed flowrate and composition is the same. This is because all the feed, no matter how it is distributed along the column, will eventually accumulate to the bottommost CS causing it to

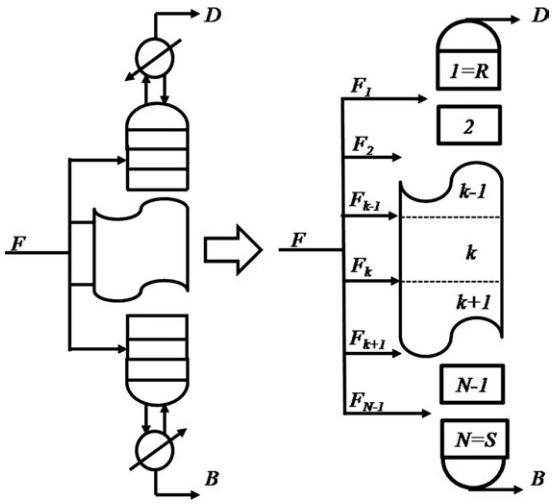

Figure 8. Typical distributed feed column with CS breakdown.

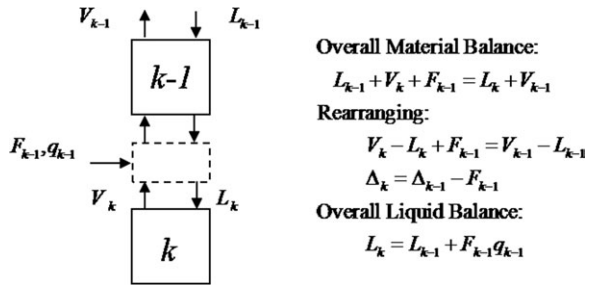

Figure 9. Magnified view of CS_k and CS_{k-1} with all stream definitions and an overall material balance.

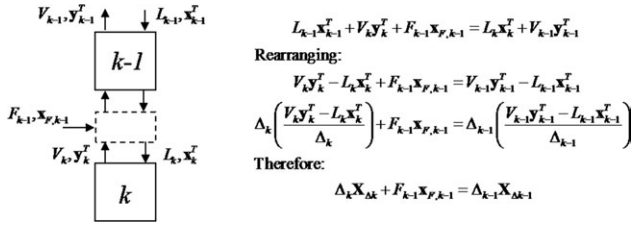

Figure 10. Magnified view of CS_{k-1} and CS_k with all stream definitions and a component balance for a generic feed.

operate at the same conditions as if all the feed has been added just above it.

Difference point effects

As mentioned, simple column design using the CPM method is much the same as boundary value method, but the CPM method's true value comes to the fore in complex columns, mainly because of the alternate placement possibilities of $\mathbf{X}_\Delta$. Consider again generalized CS_{k-1} and CS_k above and below a feed stream F_{k-1}, as shown in Figure 10 with an accompanying component balance.

The component balance in Figure 10 highlights an important result from a geometric point of view: $\mathbf{X}_\Delta$'s across a feed addition point are linearly related to the feed composition. This means that the $\mathbf{X}_\Delta$'s of adjacent CSs across a feed point, and the feed composition, will all lie on the same straight line, analogously to the bottoms, distillate and feed compositions in simple columns (Figure 5).

If adjacent CSs are in rectifying mode, the movement of the internal $\mathbf{X}_\Delta$'s tend to move outward, away from the distillate composition toward the outside of the mass balance triangle. When the point is reached where enough material has been fed to the column to change the operating mode of the CSs from rectifying to stripping, the linear trend continues, but, from the outside of the mass balance triangle inwards toward the bottoms product. This is perhaps better understood graphically, shown in Figure 11.

The extended axes of the mass balance triangle (thinner lines) depicted in Figure 11 correspond to different net compositional flow patterns. If an $\mathbf{X}_\Delta$ crosses one of these extended axes, the compositional net flow has changed in the column and a component that was moving upwards in a CS has started moving downward (or vice versa). Thus, by adjusting the feed flowrate to be sent to different points in the column, it is possible to manipulate the movement of $\mathbf{X}_\Delta$ and in so doing expose some of the interesting topology shown in Figure 7, not obtainable in simple columns.

Final design

Naturally, feed distribution brings with it additional degrees of freedom as one has to decide how the feed is to be distributed down the column. Through the overall material and component balances shown in Figures 9 and 10, both $\mathbf{X}_\Delta$ and R_Δ can be determined in each CS once the feed distribution policy has been set. Thus, all the necessary parameters for specifying the DPE completely in the internal CSs are known, and CPMs can be produced for each of these CSs. The exact location of the feed stream, generally a very difficult variable to set optimally for ternary (and higher order) systems, need not be specified and is a product of the design by simply tracing stage numbers to the point of profile intersection. The simplest case of feed distribution is deciding to divide the total feed stream into two equal sub streams. This case is shown in Figure 12 for the same base case problem depicted in Figure 6 where the simple column is at minimum column reflux. From this point, the notation $\mathbf{F_D} = [F_1, F_2, \ldots, F_N]$ is used to denote the feed distribution policy, therefore, the case of two equally divided sub feed streams and a 1 mol/s feed will be $\mathbf{F_D} = [0.5, 0.5]$.

In this case, CS_2 operates with $R_{\Delta 2} = -5.65$ and $\mathbf{X}_{\Delta 2} = [-0.68, 0.99]$. Notice that the rectifying and stripping profiles are exactly the same as those shown in Figure 6, since their boundary conditions are defined by the same product specification and column reflux. CS_2, conversely, has no set boundary condition and any of the profiles in CS_2's CPM may be utilized (green profiles). The only condition that has to be satisfied for the design to be feasible is that a continuous profile path exists between the product specifications. Notice that only the profiles contained within the bounds of CS_2's TT (dashed green lines) can result in a feasible design as only these will ensure a continuous profile path between the product specifications. This fact will be exploited in the

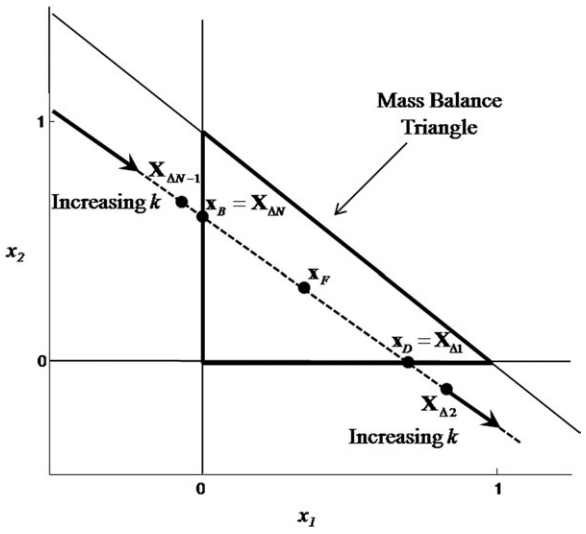

Figure 11. Movement of difference points in a distributed feed column.

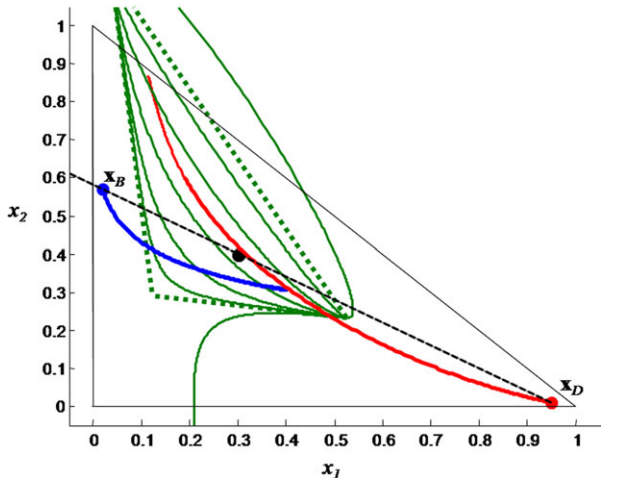

Figure 12. A distributed feed column for the base case with $\mathbf{F_D} = [0.5, 0.5]$ at $R_{\Delta R} = 2.07$.

[Color figure can be viewed in the online issue, which is available at wileyonlinelibrary.com.]

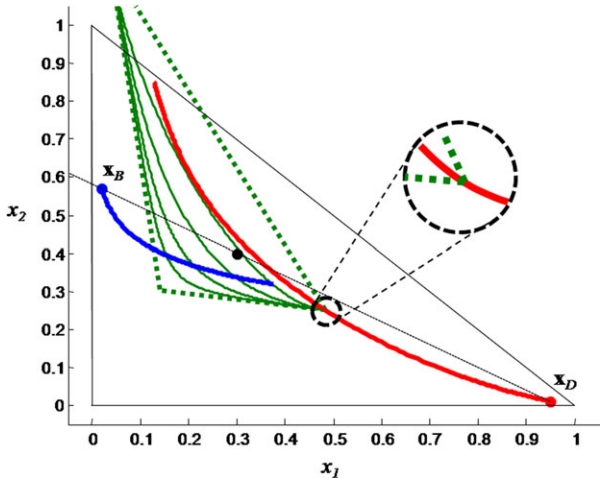

Figure 13. A distributed feed column at minimum column reflux for the base case with F_D = [0.5, 0.5] at $R_{\Delta R}$ = 1.83.

[Color figure can be viewed in the online issue, which is available at wileyonlinelibrary.com.]

discussions that follow. The specific profile in CS_2 one chooses to operate on will have a different effect on the design, as the intersection points of profiles determine the feed stages, and the total stage requirement. The intersection point between the rectifying profile and CS_2 is the location of the upper feed stage, while the intersection between the stripping CS and CS_2 represents the lower feed stage.

Benefits of Distributing the Feed

Reflux reduction

The preceding section outlined the basic design procedure for distributed feed column using the CPM technique. However, it is fair to ask whether the feed distribution actually adds any value to the base case, simple column design. Before considering whether there are benefits from a reflux point of view, it is perhaps useful to clearly state the condition for minimum column reflux: Minimum column reflux is the lowest possible reflux obtainable that will still give a continuous profile path between products and hence yield a feasible design. A column reflux below this minimum reflux implies that the product specifications cannot be met because the profile path is discontinuous. By considering the case presented in Figure 12, it is noticeable that all the possible profiles that can be used for CS_2 move past the rectifying and/or stripping profiles by some margin. It therefore follows that the minimum reflux condition for this column has not been achieved yet and, as with Figure 5, the operating conditions in this particular column are excessive. By systematically lowering the column reflux, it is possible to find this point when the vertex of CS_2's TT lies exactly on the rectifying profile, or put otherwise, where one CS has pinched on another (much the same as Figure 6). This case is presented graphically in Figure 13 where the column reflux is $R_{\Delta R} = 1.83$.

The magnified area in Figure 13 indicates that CS_2 has reached its last possible point of intersection with the rectifying profile. A further reduction in the overall column reflux will move the TT vertex of CS_2 beyond the red rectifying profile and consequently render the design infeasible because the profile path is discontinuous. Furthermore, any one of the possible operating profiles in CS_2 will be pinched, meaning the column will require an infinite number of stages. Significantly however, we have managed to drop the minimum column reflux from 2.07 in the simple column, to 1.83 in this distributed feed column—almost a 12% reduction in the minimum energy requirement of the column. This is of course not general and different degrees of savings may be achieved with different systems and feed/product specifications. Nevertheless, it is evident that distributing the feed has definite benefits from an energy perspective.

The savings shown here however leads to the question of how additional feed distribution policies will affect the reflux requirement. Consider first the same base case as discussed previously but where the feed is now divided into five equal sub feeds. Again, the minimum reflux condition is of interest and the graphical design for this is shown in Figure 14. By lowering the column reflux even more, the minimum reflux is found at $R_{\Delta R} = 1.36$, a remarkable reduction in the energy requirement of the column of nearly 35% when compared to the simple column producing the same products. Notice that the red and blue profiles representing the rectifying and stripping CSs miss each other by a considerable distance, meaning that the simple column at these operating conditions is far from being feasible.

The design in Figure 14 has four internal CSs, all of which can be used to connect product compositions with one continuous profile path. Starting from the red rectifying CS, one can "jump" onto one of CS_2's green profiles, all of which are enclosed in the green TT. From CS_2's profile, one can successively "jump" onto one of the profiles contained in the cyan, purple and gold TTs, until one reaches the blue stripping profile, taking one to the bottoms product.

In the case shown in Figure 14, the first internal CS pinches on the rectifying profile. This is however a specific case, and it is perfectly legitimate for a similar condition to occur on the stripping profile for other product distributions. It is also possible for the internal TTs not to overlap one another which will also break the continuous path between the product specifications. For the case study shown here, it turns out that the lowest minimum reflux obtainable is

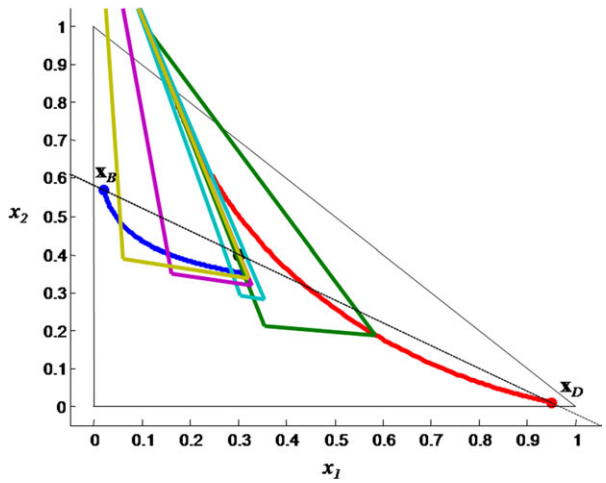

Figure 14. A distributed feed column at minimum column reflux for the base case with F_D = [0.2, 0.2, 0.2, 0.2, 0.2] at $R_{\Delta R}$ = 1.36.

[Color figure can be viewed in the online issue, which is available at wileyonlinelibrary.com.]

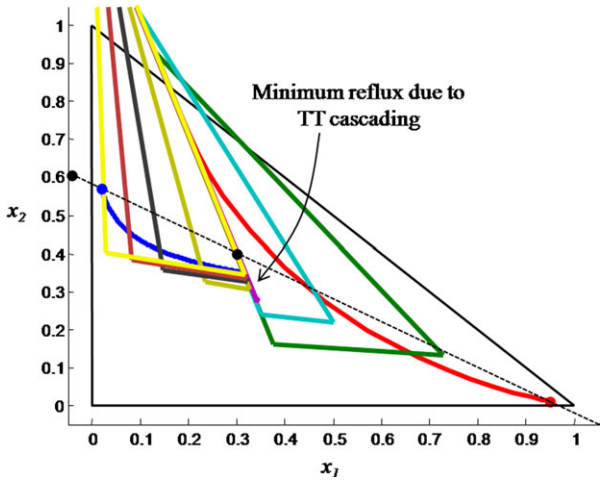

Figure 15. A distributed feed column at minimum column reflux for the base case with F_D = [0.125, 0.125, ..., 0.125, 0.125] at $R_{\Delta R}$ = 1.35.

[Color figure can be viewed in the online issue, which is available at wileyonlinelibrary.com.]

approximately $R_\Delta = 1.35$, regardless how many times the feed is (evenly) distributed. This is because the TTs of the internal CSs do not overlap any more at column refluxes lower than 1.35, as shown in Figure 15 where the feed has been distributed eight times. Notice that this choice of column reflux causes the TTs of the internal CSs to cascade around the same line, indicating the last point of intersection. If one were to reduce the column reflux any further, there would be no overlapping of these TTs and the column would be infeasible irrespective of how many times the feed is distributed. Additional feed distributions simply result in the same cascading effect shown in Figure 15. $R_{\Delta R} = 1.35$ is thus the minimum distributed feed reflux for this column. In most cases investigated by the authors, the majority of the savings is gained by the first five feed distributions, and any further feed distributions has little to no effect on the minimum column reflux.

Stage reduction

As mentioned previously, minimum reflux is not a practical operating condition since the stage numbers tend towards infinity in a particular CS as it nears its stationary point. General guidelines in distillation generally recommend operating slightly above minimum reflux, usually by a factor of 1.05–1.5, depending on the system.[34] Operating at this elevated column reflux means that a pinched CS at minimum reflux requiring an infinite number of stages is now further from its stationary point, and the column makes sense from an economic point of view because a finite sized column can be built. There is however a trade-off between the energy (reflux) and capital (number of stages) of the column. It is evident that one would like to avoid areas on profiles that are near stationary points as the stage numbering is very dense in these areas resulting in large columns. The distributed feed column is useful for stage reduction too, because it allows one to "jump" past an area of infinite stages using the internal CS. To illustrate this, consider the minimum reflux simple column shown in Figure 6 operating at $R_{\Delta R} = 2.07$. If one decides to distribute the feed equally into two sub-feeds at the simple column's minimum reflux ($R_{\Delta R} = 2.07$), a design shown in Figure 16 can be obtained.

Figure 16 shows that the green, un-pinched profile allows one to move around the pinched profile of the stripping CS. Thus, this separation can be achieved at the minimum reflux of the simple column but with a finite number of stages. In a sense, this result is automatic, because if a reduction in reflux can be achieved (as shown in the previous section) then a stage reduction can also be achieved since these variables are inextricably linked to one another. It has been shown that the $\mathbf{F_D}$ = [0.5, 0.5] column (Figure 13) can achieve a minimum reflux of 1.83 (requiring an infinite number of stages), and, thus, the design shown in Figure 16 is simply a situation above that minimum reflux requiring a finite number of stages.

Sidestream withdrawal flexibility

Sampling an intermediate product from a column may be desired in certain scenarios. Drawing a significant amount of sidestream product from a distillation column will intuitively affect the reflux ratios in subsequent CSs. These additional reflux effects are easy to calculate, but for ease of understanding and brevity, it will assumed that only an infinitesimal amount of sidestream product is being drawn from the column, meaning that reflux ratio calculations remain unaffected. With this in mind, consider again the profiles of the simple column depicted in Figure 5. It is easy to comprehend that any composition along either the rectifying of stripping CS's profile is a potential sidestream composition that may be sampled along the length of the column. It merely depends on how far up in the column, that is, on which stage, the sidestream is sampled. If one now operates at the same minimum column reflux as the simple column ($R_{\Delta R} = 2.07$), but decides to distribute the feed into infinitely many sub streams, it is possible to construct an entire region of potential side-draw compositions, as shown in Figure 17.

The green region in Figure 17 represents all possible compositions that may be sampled in a sidestream, a significant expansion of possible sidestream compositions attainable in the simple column. The region was constructed by simply choosing a feed distribution policy that requires an infinitesimal addition of material at each feed entry point. For each

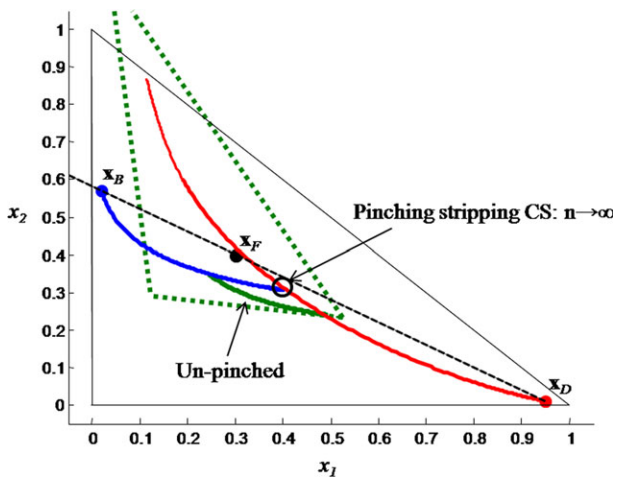

Figure 16. A distributed feed column for the base case with F_D = [0.5, 0.5] at $R_{\Delta R}$ = 2.07, where the pinched area has been avoided.

[Color figure can be viewed in the online issue, which is available at wileyonlinelibrary.com.]

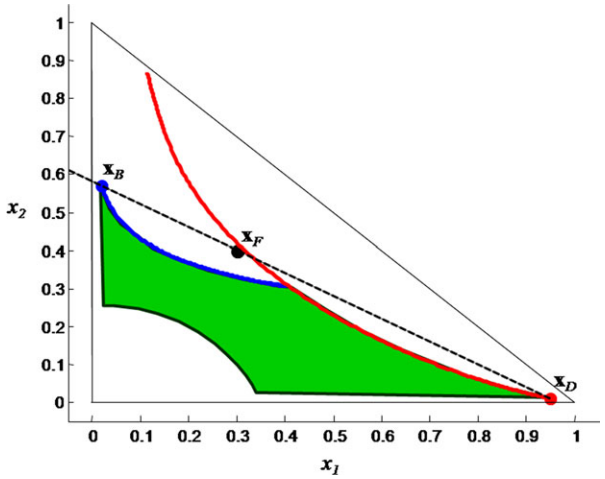

Figure 17. A infinitely distributed feed column for the base case with $R_{\Delta R}$ = 2.07.

[Color figure can be viewed in the online issue, which is available at wileyonlinelibrary.com.]

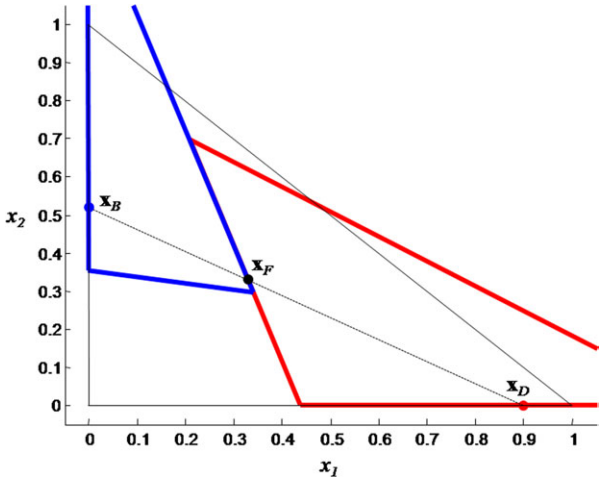

Figure 18. A sharp split minimum reflux design using TTs at $R_{\Delta R}$ = 1.07.

[Color figure can be viewed in the online issue, which is available at wileyonlinelibrary.com.]

resulting CS that has been created by this feed policy, a TT is produced which allows on to infer the region in Figure 17. The curvature of the bottom-left part of this region is a locus of the saddle point vertices of the TTs of the internal CSs (notice sidestream a similar TT trend in Figure 14 and Figure 15). Any sidestream composition within this region can be obtained with some sort of feed distribution policy and combination of profiles. Perhaps more importantly however is that compositions not within the green region can never be obtained, regardless of the feed distribution policy. The green region therefore places a limit on possible sidedraw compositions.

Feasibility

A noticeable point in some of the distributed feed columns that have been designed thus far (particularly Figures 12 and 14), is that the simple column profiles at these reduced reflux ratios are in fact missing one another, although the distributed feed design is still feasible. Viewed from another perspective, feed distribution has the power to make apparent infeasible columns, feasible. Now this may not have a significant impact on ideal systems, since feasibility is quite well understood in these systems, but it may have a significant impact on non-ideal systems containing azeotropes and distillation boundaries, as shown in Figure 7. As the intention of this article is only to highlight the benefits of feed distribution, a detailed design of a non-ideal systems using feed distribution is not shown here but will be addressed in future presentations. At this point, the reader should simply be aware that feed distribution has the potential to positively alter the feasibility of an azeotropic column.

Limitations

Sharp splits

Although it seems as though feed distribution is an easy means of obtaining significant reductions in energy consumption and stage numbers requirements, it does have limitations specifically pertaining to sharp splits, that is, when product compositions lie on the edges of the mass balance triangle, or in other words, at least one component is non-distributing. Sharp split, simple column design is quite easy using the CPM technique as one does not even need to integrate the DPE, but merely plot the TTs of the rectifying and stripping CSs.[17,21] When these TTs become co-linear, a minimum reflux design has been found. Solutions found for minimum reflux using this technique are in fact exactly the same as those found through the classic Underwood equations.[35] This is illustrated in Figure 18 for the design where $\mathbf{x}_F$ = [0.33, 0.33], $\mathbf{x}_D$ = [0.9, 0], and $\mathbf{x}_B$ = [0, 0.521] and a pure liquid feed. The minimum reflux is found to be 1.07.

The system in Figure 18 is feasible since there is a continuous profile path between products, albeit that this path lies on the edge of the TTs and hence requires an infinite number of stages (both profiles have to run precisely through their respective saddle nodes). Any reduction in the column reflux above would violate the condition of a continuous profile path because the TTs will miss each other. Now, for the same column at the same column reflux ratio as in Figure 18, it is arbitrarily chosen to distribute the feed into three equal streams. Using the TTs, as shown in Figure 19, it is again possible to analyze the influence of distributed feed.

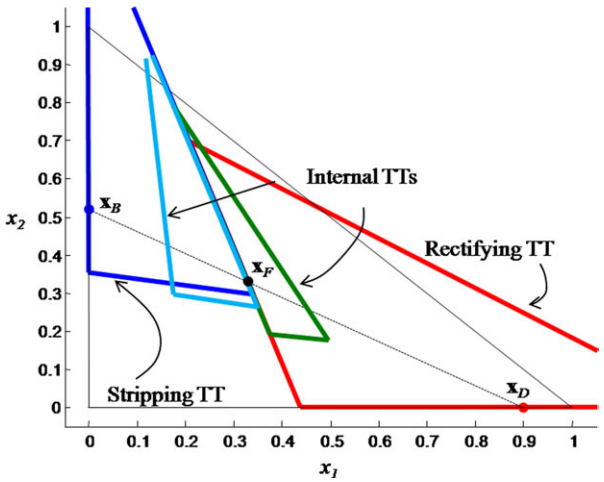

Figure 19. A sharp split distributed feed design at minimum reflux using TTs at $R_{\Delta R}$ = 1.07.

[Color figure can be viewed in the online issue, which is available at wileyonlinelibrary.com.]

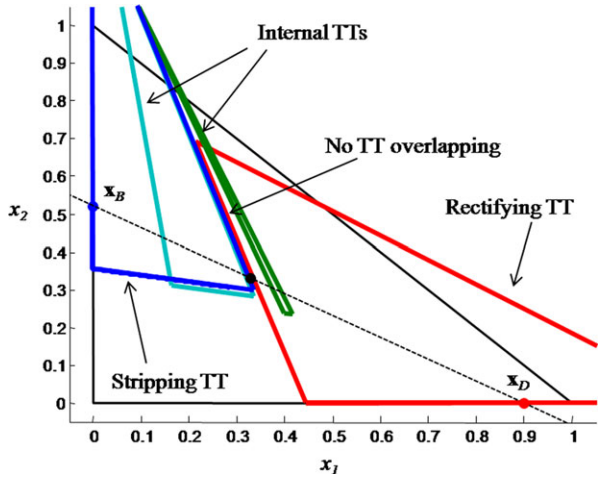

Figure 20. An infeasible distributed feed column at $R_{\Delta R} = 1.05$.

[Color figure can be viewed in the online issue, which is available at wileyonlinelibrary.com.]

Figure 19 points out at that there is in fact no advantage to be gained by distributing the feed at sharp split conditions. This condition arises because the green and cyan TTs (the TTs for the internal CSs) are colinear along the same line as the blue and red TTs are for the simple column, similarly to the design in Figure 15. Thus, the minimum reflux of the simple column is also the lowest minimum reflux achievable in the distributed feed column if the desired product distribution is sharp. If a column reflux below the simple column minimum reflux is chosen, the green and cyan TT will not overlap at all and the design will not be feasible because the profile path between product specifications is broken, as shown in Figure 20.

Because of the fact that the TT technique is equivalent to the Underwood method for minimum reflux at sharp split conditions, distributed feed calculations using Underwood's method will show that there are no benefits to feed distribution. As the Underwood technique has been widely used for shortcut distillation calculations, it offers a partial explanation as to why the distributed column has received so little attention in the literature. This of course raises the question about how sharp is a sharp split, or alternatively, does moving further away from sharp split conditions result in additional savings? These are not necessarily straightforward questions to answer as it is system specific, and will be addressed in a future publication.

Binary mixtures

Binary distillation columns have traditionally been designed, at least for first approximations, using the McCabe-Thiele method. It is important to realize that the binary distillation problem is in fact a sharp split problem from a geometric perspective because the products are constrained to lie on the axes if the mass balance triangle. It therefore follows that binary distillation has the same limitations with regard to feed distributions as sharp split problems. In the case shown below, a constant volatility of 2.5 has been assumed between component x_1 and x_3 with a binary liquid feed of $\mathbf{x}_F = [0.5, 0]$, and products of $\mathbf{x}_D = [0.99, 0]$, $\mathbf{x}_B = [0.02, 0]$. The simple column minimum reflux is easily obtained as $R_{\Delta R} = 1.29$ for these design specifications, and profiles at these conditions have been plotted in Figure 21. Although this is a binary problem (notice the absence of component x_2 in the feed and products), it has been described from a ternary CPM perspective such that TTs can be used for visualization.

An interesting, but well known, aspect of binary distillation is that that rectifying and stripping profiles pinch simultaneously at the feed composition at minimum reflux. It is then again evident from Figure 21 that feed distribution does not offer advantages because the internal CSs' TTs simply cascade around the pinch points of the rectifying and stripping CSs at the feed composition. Any reduction of the column reflux below the simple column reflux thus results in an infeasible column, irrespective of the feed addition mechanism. This result can be shown very easily with the McCabe-Thiele method. This may again offer an explanation to the under-utilization of distributed feed because the McCabe-Thiele method is incapable of recognizing the aforementioned advantages due to the method's restriction to binary mixtures only.

Feed placement

Finally, a potential disadvantage/problem from an operational point of view with a feed distribution policy may be that, once a set of operating profiles has been selected, each profile intersection, that is, feed stage has to be exactly satisfied. For instance, in the column design shown in Figure 16, the feed stage requirements of both the red-green and blue-green profile intersections have to be simultaneously met, or the design may not be feasible. Remember that there are a plethora of profiles that one may choose for the internal CSs, but each profile one elects, although still feasible, will have different feed stage placements. This problem is compounded even more when the number of feed distributions increases as multiple feed stages need to be found and satisfied. In short, it may be difficult to add the feed exactly at the place required for the design to be feasible and product specifications to be met. This will become apparent in the following section on validation through Aspen Plus®. Nevertheless, this problem is thought not be insurmountable and may be overcome through control or a design flexibility analysis, or by constructing a packed column which allows feed addition at virtually any point along the column length.

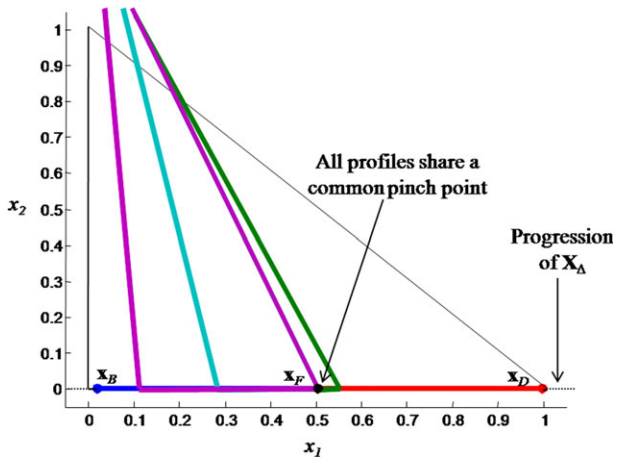

Figure 21. A binary distributed feed design at minimum reflux using TTs.

[Color figure can be viewed in the online issue, which is available at wileyonlinelibrary.com.]

Validation with Aspen Plus

The results shown in this article thus far indicate that there are significant benefits to feed distribution. However, for the results to be conclusive and to be certain that they are not merely products of the method, it is necessary to validate the findings with a widely accepted simulation package. For this purpose Aspen Plus'® Radfrac column is used, which rigorously calculates compositions on each equilibrium stage and product stream through tray-by-tray mass, equilibrium, summation, and heat equations. This calculation does not assume constant molar overflow as the DPE does. The Radfrac simulation model requires that the user specifies a distillate flowrate, the column reflux ratio, the total number of equilibrium stages, and the location of each feed stage. Once the equations have successfully converged, the user can obtain the final product compositions and of course the compositions on each equilibrium stage. The fundamental difference between the CPM/boundary value method and the Radfrac model is that in the Radfrac model, product compositions are a result of a certain prespecified column internals (total number of stages, feed stages, etc.) whereas the CPM/boundary value method gives the column structure [number of stages, feed stage(s)] as a result of prespecified product compositions.

For the validation, the real Benzene, p-Xylene, Toluene system has been chosen using the NRTL model for phase equilibrium calculations. The following feed and product specifications will be imposed upon on the design (compositions are given in the form [Benzene, p-Xylene]): $F = 1$ mol/s, $q = 1$ (liquid feed), $\mathbf{x}_F = [0.3, 0.3]$, $\mathbf{x}_D = [0.9, 0.01]$, and $\mathbf{x}_B = [0.01, 0.44]$. From these specifications, one can easily determine by mass balance that $D = 0.32584$ mol/s and $B = 0.67416$ mol/s. It is very important to note that these product compositions should be met exactly, or as closely possible. For instance, a column producing no p-Xylene in the distillate is undesirable; we would in fact like the specification of 0.01 for this component to be met as strictly possible. This holds for all components in the product streams.

Using the CPM approach, it is then possible to obtain the design with the red and blue profiles in Figure 22 at a reflux of 1.76. The true minimum reflux of this column is actually 1.75, but a slightly higher reflux value has been chosen such that a finite sized column can be obtained. By tracing the stage numbers on each profile, the total number of stages is determined to be 27.78 (where the partial reboiler acts as an equilibrium stage), and the feed stage to be 4.75 from the top (when counting from 1). Note that the stage numbers are non-integer, and can be viewed as the position coordinate in a packed column. It will however be shown that these values correspond extremely well to discrete, staged columns. To validate this design, the following data is transported into Aspen Plus®'s Radfrac column: Distillate flowrate = 0.32584 mol/s, column reflux ratio = 1.76, a kettle reboiler, a total condenser, total number of equilibrium stages = 27 (since reboiler acts as a stage, the actual column requires 26.78 stages but is rounded to 27), and the feed stage at stage 5 (also rounded, and specified to be "On-Stage"). The feed stream was taken to be 1 mol/s and a pure liquid at 1 atm pressure. The same NRTL model was also used for the Aspen Plus® calculations (see Appendix A for a detailed list of all parameters used in both the CPM and Aspen Plus® designs). The Radfrac block is now completely specified and upon allowing the simulator to converge, the compositions

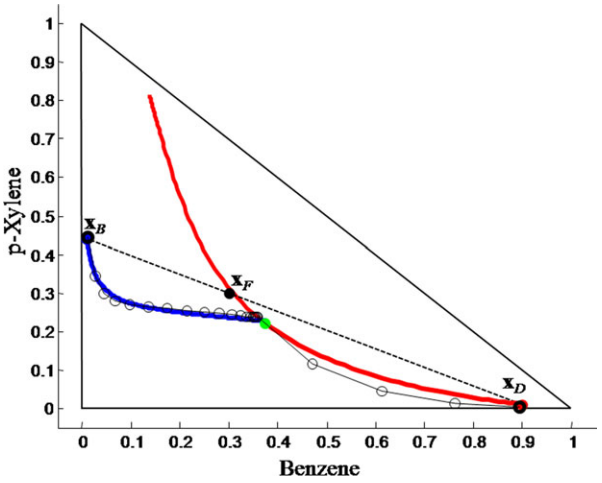

Figure 22. A feasible simple column for the Benzene, p-Xylene, Toluene system showing the CPM profiles (red and blue) and a design from Aspen Plus® initialized using CPM values (black).

Product compositions predicted by Aspen Plus® are outlined thicker. [Color figure can be viewed in the online issue, which is available at wileyonlinelibrary.com.]

on each stage and products stream is extracted and superimposed on the CPM design in Figure 22.

It is evident from Figure 22 that the CPM profiles and Aspen Plus® predictions match quite closely. The product compositions predicted by Aspen Plus® are outlined with a thicker line to indicate their proximity to the actual CPM specifications. The exact product compositions predicted by Aspen Plus® are: $\mathbf{x}_D = [0.9046, 0.0018]$, $\mathbf{x}_B = [0.0078, 0.4441]$.

However, it can be seen that the aforementioned Aspen Plus® product composition are not exactly equal to the prespecified product compositions. To quantify the deviation of the calculated product specifications to those specified, a sum of squared errors function is used i.e.

$$f = \sqrt{\sum_{i=1}^{3}\left(x_{Di,\text{Aspen}} - x_{Di,\text{Spec}}\right)^2 + \sum_{i=1}^{3}\left(x_{Bi,\text{Aspen}} - x_{Bi,\text{Spec}}\right)^2} \tag{5}$$

In Eq. 5, the notation $x_{Di,\text{Aspen}}$ represents the distillate composition of component i predicted by Aspen Plus®, while $x_{Di,\text{Spec}}$ represents the desired product specification of component i in the distillate. An analogous notation is used for the bottoms compositions. Furthermore, to eliminate bias to certain compositions and give equal importance to each of the desired specifications, the normalised sum of squared errors in Eq. 6 is also used

$$g = \sqrt{\sum_{i=1}^{3}\left(\frac{x_{Di,\text{Aspen}} - x_{Di,\text{Spec}}}{x_{Di,\text{Spec}}}\right)^2 + \sum_{i=1}^{3}\left(\frac{x_{Bi,\text{Aspen}} - x_{Bi,\text{Spec}}}{x_{Bi,\text{Spec}}}\right)^2} \tag{6}$$

Both functions f and g will provide a measure of the proximity of the calculated product compositions to the prespecified compositions. For the case shown in Figure 22, the

Table 1. Comparison of Optimized Simple Column Objective Function and Reflux Ratio

Objective Function	Optimized Reflux	Function Value
f	1.889	0.0111
g	1.827	0.8071

Aspen Plus® product compositions gave rise to values for f and g of 0.0111 and 0.8464, respectively. Although the design in Aspen Plus® is quite close to the one predicted by the CPM method, it is wished that an optimal Aspen Plus® base case is established for the simple column. Thus, an optimization routine was run in Aspen Plus® which minimizes either one of the objective functions in Eqs. 5 and 6 using the column reflux as the varied parameter. Table 1 summarizes these results.

Table 1 shows that the optimized function values are in fact not that different to those obtained by directly inserting the CPM predicted column reflux values. The optimized reflux ratio for function g is only about 4% different than the original CPM prediction, while the optimized reflux ratio for function f is about 7% different (even though f's objective function value is different by less than 10^{-4}!). These slight differences may be attributed to the constant molar overflow assumption of CPMs, or by the fact it is impossible to specify the exact feed stage which the CPM method predicts (4.75) within Aspen Plus®. Importantly, it can be seen that the CPM method serves as a very useful initialization technique for Aspen Plus®.

For the purpose of comparison, the reflux and function values of f and g in Table 1 will be used as the base case for Aspen Plus® comparisons. In all subsequent designs, the reflux ratio will be considered the important variable to be improved upon. For any design to be classed as better as the base cases in Table 1, the function value should be smaller (products compositions lie closer to their specified values) and the reflux requirement should be less, given the same number of equilibrium stages.

Furthermore, before considering the distributed feed case, it is important to be certain that the optimal feed stage has been obtained for the simple column, as this severely influences the final product purity. Figures 23a, b illustrate the minimum value of the objective functions f and g, respectively, vs. the optimized reflux ratio that yields this minimum objective function for different feed stage cases in the simple column. All cases in Figures 23a, b have a total of 27 equilibrium stages. Clearly, the chosen base case (feed stage = 5) simultaneously results in the lowest reflux and objective function values. In Figure 23a, b, and for all subsequent designs, a design is only considered better than the base case if and only if it lies within the so-called "Region of Improvement." If a design lies within this region, then both a lower reflux and closer proximity to the exact product specifications have been achieved. The "CPM value" illustrates the case where the reflux found via the CPM method was inserted directly into Aspen Plus® with no optimization routine.

Now that the best simple column design to produce the predefined products has been convincingly found, it is possible to focus on whether feed distribution can improve on this base case. By first considering the simplest case, a double feed column with two equal feed distributions, the CPM method predicts the design shown in Figure 24. In performing this design using CPMs, a conscious effort was made to keep the total number of stages approximately the same as the base case such that a fair comparison can be made. This can be done by carefully selecting an appropriate profile in the internal CS (shown by the thick, green profile). In Figure 24, the design requires 26.55 total stages, with the first feed stage located at 4.42 and the second feed stage at 13.33. Using the CPM method, the overall column reflux is found to be 1.6, a reduction of approximately 9% in the energy usage of the column. Note that this is not the minimum reflux of the column; it is merely a reflux that has been found that will keep the total number of equilibrium stages at approximately 27.

As with the simple column it is now possible to transport the CPM predictions into the rigorous Radfrac block in Aspen Plus®. The same Radfrac column used for the simple column validation is used again, except that the column is specified to have two feed entry points (rounded to stages 4 and 13, "On-Stage"), with both feed streams being equal with a flowrate of 0.5 mol/s each. The same optimization routine in Aspen Plus® is used once more, that is, a column reflux has to be found that minimizes the objective functions

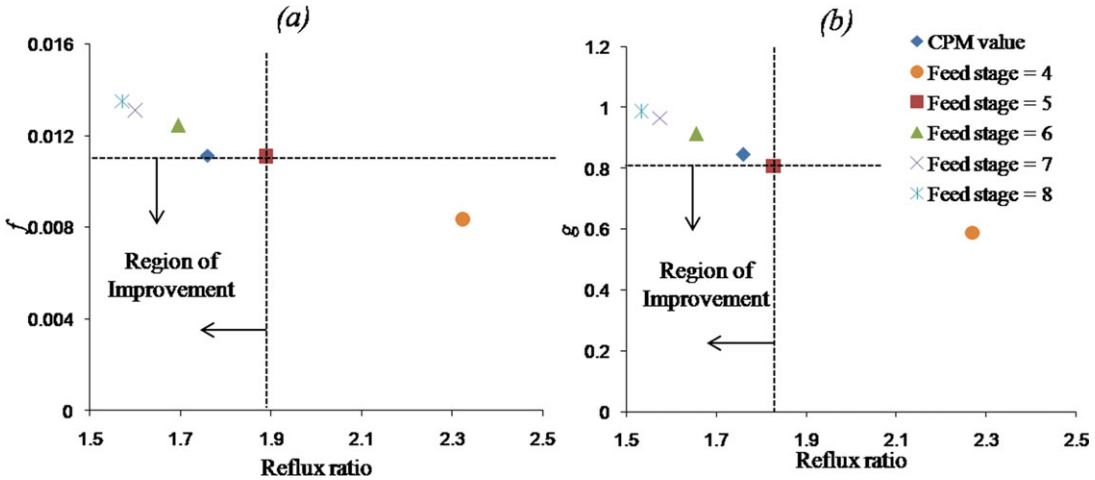

Figure 23. The effect of the feed stage location in a simple column on: (a) minimized objective function f vs. optimized reflux ratio, and (b) minimized objective function g vs. optimized reflux ratio.

[Color figure can be viewed in the online issue, which is available at wileyonlinelibrary.com.]

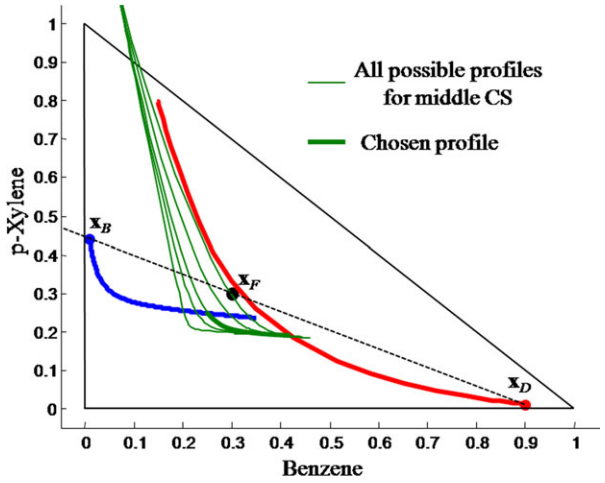

Figure 24. A distributed feed column for Benzene, p-Xylene, Toluene system with F_D = [0.5, 0.5] at $R_{\Delta R}$ = 1.6.

[Color figure can be viewed in the online issue, which is available at wileyonlinelibrary.com.]

f and g. Furthermore, one should first consider that the optimal combination of feed stage locations predicted by the CPM method may be slightly different than the optimal combination found by Aspen Plus®. Thus, the same optimization procedure was performed with different feed stage combinations. The first feed stage was chosen to be on either stage 3, 4, or 5, while the second feed stage was chosen to lie on 12, 13, or 14 (either side of the rounded CPM predictions in both cases). In all, 9 different double feed configurations were considered. Figures 25a, b illustrates the properties of each of these cases on an objective function versus optimal reflux plot. The first feed entry point is represented by a blue, red, and green marker for stages 3, 4, and 5, respectively, while the second feed entry point is represented by a cross, square, and triangular marker for stages 12, 13, and 14, respectively. The legend is in the form (i,j), indicating that the feed stage one is located on stage i and the second feed stage on stage j.

Figures 25a, b clearly shows that feed distribution offers an advantage to the optimal single feed case, as all red markers are grouped within the "Region of Improvement" governed by the base case in Figure 23a, b. These cases all represent columns where the first feed stage is at stage 4, and the second feed stage is at either stage 12, 13, or 14. It is worthwhile to point out that both objective functions have almost identical trends, although the exact values of the optimal reflux are slightly different. Moreover, it can be seen that the first feed entry point severely affects the design, but the second feed stage has almost no influence at all. As discussed in the section on feed placement, matching the feed stages with one another may prove to be challenging. For instance, in this configuration, by erroneously selecting the first feed entry point, the design may well be considerably worse than the best simple column. Again, the CPM predictions serve as a useful method to target the optimal feed stage locations.

In the case of both objective functions, it turns out that the lowest achievable reflux within the "Region of Improvement" is when the feed is distributed to stages 4 and 14. In this case, using objective function f, the optimal reflux is found to be 1.765 (compared to the optimal single feed case of 1.889), resulting in a saving of 6.55%. For objective function g, the optimal reflux is 1.740, resulting in a saving of 4.74% (when compared to the optimal single feed case of 1.827). Although the savings are not quite as dramatic as predicted by the CPM method, it is thought the Aspen Plus® results are still suboptimal since the feed stage is restricted to be integer-only. If a packed column were used, for instance, it may be possible to feed the column on the equivalent of stage 4.55 (as predicted by the CPM method), that is, somewhere between stage 4 and 5 that will allow one to obtain a lower reflux and still satisfy the objective function. Nevertheless, it has been demonstrated that there are definite advantages to feed distribution. Figure 26 shows CPM profiles for the distributed feed case (at $R_{\Delta R}$ = 1.6), superimposed upon the optimal predictions of Aspen Plus® discussed above and summarized in Table 2.

As with the simple column in Figure 22, Figure 26 also demonstrates a remarkable similarity between the Aspen Plus® profiles and those from the CPM method. It can be seen that the two Aspen Plus® profiles are virtually identical. Table 2 summarizes optimal cases generated for 1, 2, 3, and 4 feed columns using Aspen Plus®. All data in Table 2 have been generated using the same optimization procedure outlined previously, and with initialization values from the CPM method. Note that the 3 and 4 feed cases result in substantial reflux savings while still satisfying the objective function value.

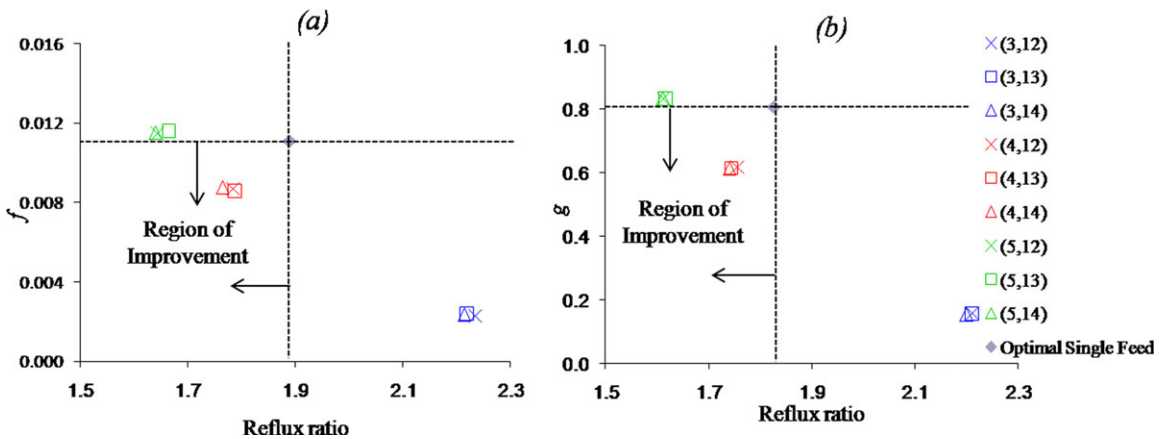

Figure 25. The effect of the feed stage location in a distributed feed column on: (a) minimized objective function f vs. optimized reflux ratio, and (b) minimized objective function g vs. optimized reflux ratio.

[Color figure can be viewed in the online issue, which is available at wileyonlinelibrary.com.]

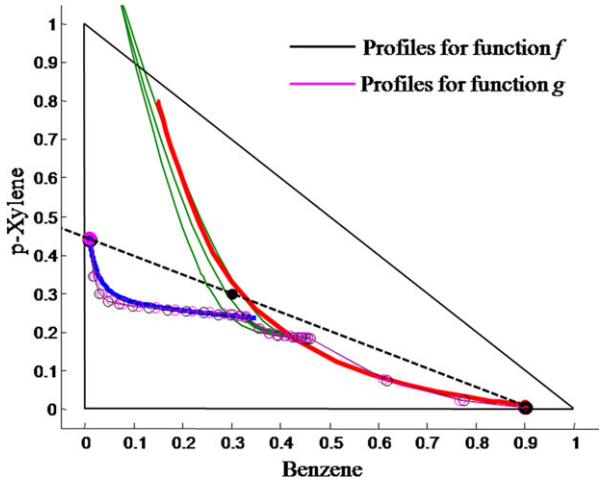

Figure 26. A feasible distributed feed column for the Benzene, p-Xylene, Toluene system showing the CPM profiles (red and blue), and a design from Aspen Plus® using *f* and *g* as objective functions (black and purple profiles, respectively).

Product compositions predicted by Aspen Plus® are outlined thicker. [Color figure can be viewed in the online issue, which is available at wileyonlinelibrary.com.]

Again, the trend shown in Table 2 agrees very well with the CPM predictions: additional feed distributions lead to greater savings, up to a certain limit. It is evident that the savings begin to plateau after 4 distributions. It should again be emphasized that all the designs shown in Table 2 require a total of 27 stages. The reader should also be aware that finding these configurations can be very difficult if one does not have good initialization procedures. An important outcome of this section is to show that the CPM predictions are reasonably accurate and can aid in finding designs in Aspen Plus® much easier, and in a systematic fashion. Trying to simultaneously compute the total number of stages, required reflux, feed entry points, and product flowrates that will yield a certain product distribution by relying solely on Aspen Plus®, is likely to be very challenging and time- consuming.

Discussion and Conclusions

This article presents the design and analysis of distributed feed columns using the CPM technique. The CPM method is shown to be an extremely insightful design tool as it allows the designer to utilize interesting and useful mathematical/topographical characteristics by not bounding the designer to any pre-conceived structures. Complex columns, such as the distributed feed column presented here, are very useful in this regard because they permit these potentially useful topological traits.

Specifically, it is shown here how useful information can be gained in the design of distributed feed columns using geometrical phenomena like TTs for ideal systems. Using the CPM technique it is easy to estimate minimum reflux for a distributed feed column. The designs shown in this article indicate that feed distribution offers significant advantages over so-called simple columns from both an energy and a stage requirement point of view. The CPM case study shown in the section on reflux reduction suggests savings in the order of 35% if the column is designed optimally.

Although the feed distribution policy may hold significant advantages, it is not necessarily applicable to all separations. Specifically, binary mixtures and sharp split problems are not good candidates for feed distribution since there is no advantage to be gained in either case. As these cases are the most frequently taught and studied cases in distillation (through the Underwood and McCabe-Thiele methods), it is difficult to recognize the advantages of feed distribution without using a generalized CPM-type approach.

This article only addresses evenly distributed feed columns. In other words, the global feed stream is divided into equal parts and fed at different points along the length of the column. There are of course many other scenarios that may be considered such as uneven distribution of the feed, feeds with different compositions, or feeds with different thermodynamic states (liquid or vapour, or a mixture). Furthermore, this paper only addresses the simplest case of feed distribution, that is, on a simple column. It is expected that there are similar savings to be realized if a feed distribution policy were to be applied to complex columns such as Petlyuk columns, which already represent substantial energy savings. All these aforementioned scenarios are very straightforward to implement into the current CPM design methodology and will be the topic of future publications.

Finally, and perhaps most importantly, this article shows a case study for the real Benzene, p-Xylene, Toluene system, whereby design targets were obtained using the CPM method and subsequently implemented into Aspen Plus®. To a large extent, the Aspen Plus® and CPM designs agree very well with one another. Importantly, using an objective function to ensure that the product distribution is met as close as possible, Aspen Plus® optimization results yield the same trend of reflux savings for feed distribution that the CPM method predicts. Although savings with Aspen Plus® have been demonstrated, it is thought that these results may still be suboptimal because the feed entry points are required to lie on integer-numbered stages, and not on a continuous position along the column length, but this may well be overcome using a packed column.

Finally, the authors would like to point out that the key to understanding these counter-intuitive results is the use of the *f* and *g* functions which are used to assess the improvement (reduction) in the energy consumption and the proximity to the desired product specification. The use of objective functions *f* and *g* are a very unique means of assessing the performance of a column, and the reader should bear this in mind when comparing the method (and the claimed savings) to more conventional means of design. The authors realize that these results in this paper go against virtually all understood principles of distillation, because it has generally been

Table 2. Comparison of Optimized Simple Column Objective Function and Reflux Ratio

Number of Feeds	Feed Stage(s)	Objective Function	Optimized Reflux	Reflux Savings (%)	Function Value
1	(5)	*f*	1.889	–	0.0111
1	(5)	*g*	1.827	–	0.8071
2	(4,14)	*f*	1.765	6.55	0.0088
2	(4,14)	*g*	1.740	4.74	0.6139
3	(4,13,18)	*f*	1.652	12.54	0.0096
3	(4,13,18)	*g*	1.624	11.11	0.6703
4	(4,12,15,18)	*f*	1.626	13.92	0.0102
4	(4,12,15,18)	*g*	1.603	12.22	0.7211

thought that splitting the feed dilutes the composition on the stages and so that should lead to an increase in the separation effort required by the column (either an increase in reflux or stage requirement). This belief may very well hold true in certain cases, such as sharp split designs. However, the authors believe that, although the design procedure shown here is somewhat unconventional, the results are quite resounding and conclusive, and certainly warrants a relook at current distillation design principles.

Literature Cited

1. Soave G, Feliu JA. Saving energy in distillation towers by feed splitting. *Appl Therm Eng*. 2002;22:889–896.
2. McCabe WL, Thiele EW. Graphical Design of Fractionating Columns. *Ind Eng Chem*. 1925;17:606–611.
3. Van Dongen DB, Doherty MF. Design and synthesis of homogeneous azeotropic distillations. 1. Problem formulation for a single column. *Ind Eng Chem Fundam*. 1985;24:454–463.
4. Doherty MF, Caldarola GA. Design and synthesis of homogeneous azeotropic distillations. 3. The sequencing of columns for azeotropic and extractive distillations. *Ind Eng Chem Fundam*. 1985;24:474–485.
5. Levy SG, Van Dongen DB, Doherty MF. Design and Synthesis of homogeneous azeotropic distillations. 2. Minimum reflux calculations for nonideal and azeotropic columns. *Ind Eng Chem Fundam*. 1985;24:463–474.
6. Zhang L, Linninger AA. Temperature collocation algorithm for fast and robust distillation design. *Ind Eng Chem Res*. 2004;43:3163–3182.
7. Lucia A, Amale A, Taylor R. Energy efficient hybrid separation processes. *Ind Eng Chem Res*. 2006;45:8319–8328.
8. Lucia A, McCallum BR. Energy targeting and minimum energy distillation column sequences. *Comput Chem Eng*. 2010;34:931–942.
9. Petlyuk FB, Platonov VM, Slavinskii DM. Thermodynamically optimal method for separating multicomponent mixtures. *Int Chem Eng*. 1965;5:554–561.
10. Lucia A, Amale A, Taylor R. Distillation pinch points and more. *Comput Chem Eng*. 2008;32:1342–1364.
11. Halvorsen IJ, Skogestad S. Optimizing control of Petlyuk distillation: understanding the steady-state behavior. *Comput Chem Eng*. 1997;21(Supplement 1):S249–S254.
12. Agrawal R, Fidkowski ZT. Are thermally coupled distillation columns always thermodynamically more efficient for ternary distillations? *Ind Eng Chem Res*. 1998;37:3444–3454.
13. Backhaus AA, Inventor. Apparatus for producing high grade esters. US Patent 14032241922.
14. Halvorsen IJ, Skogestad S. Minimum energy consumption in multicomponent distillation. 2. Three-product Petlyuk arrangements. *Ind Eng Chem Res*. 2003;42:605–615.
15. Alstad V, Halvorsen IJ, Skogestad S. *Optimal operation of a Petlyuk distillation column: energy savings by over-fractionating*. In: Barbosa-Póvoa A, Matos H, editors. *Computer Aided Chemical Engineering*, Vol. 18: Elsevier, 2004;547–552.
16. Segovia-Hernández JG, Hernández S, Jiménez A. Analysis of dynamic properties of alternative sequences to the Petlyuk column. *Comput Chem Eng*. 2005;29:1389–1399.
17. Holland ST, Abbas R, Hildebrandt D, Glasser D. Complex column design by application of column profile map techniques: sharp-split Petlyuk column design. *Ind Eng Chem Res*. 2010;49:327–349.
18. Holland ST, Tapp M, Hildebrandt D, Glasser D. Column profile maps. 2. Singular points and phase diagram behaviour in ideal and nonideal systems. *Ind Eng Chem Res*. 2004;43:3590–3603.
19. Tapp M, Holland ST, Hildebrandt D, Glasser D. Column profile maps. 1. Derivation and interpretation. *Ind Eng Chem Res*. 2004;43:364–374.
20. Hömmerich U, Rautenbach R. Design and optimization of combined pervaporation/distillation processes for the production of MTBE. *J Membr Sci*. 1998;146:53–64.
21. Holland ST, Tapp M, Hildebrandt D, Glasser D, Hausberger B. Novel separation system design using "moving triangles." *Comput Chem Eng*. 2004;29:181–189.
22. Rautenbach R, Albrecht R. *Membrane Processes*, 1 ed. New York: Wiley, 1989.
23. Levy SG, Doherty MF. Design and synthesis of homogeneous azeotropic distillations. 4. Minimum reflux calculations for multiple-feed columns. *Ind Eng Chem Fundam*. 1986;25:269–279.
24. Peters M, Hildebrandt D, Glasser D, Kauchali S. *Membrane Process Design Using Residue Curve Maps*. New York: Wiley, 2011.
25. Humphrey JL. Separation processes: playing a critical role. *Chem Eng Progr*. 1995;91:31–41.
26. Towler G, Sinnott R. *Chemical Engineering Design: Principles, Practice and Economics of Plant and Process Design*. London, UK.: Elsevier, 2007.
27. Holland ST. *Column Profile Maps: A Tool for the Design and Analysis of Complex Distillation Systems*. Johannesburg: Chemical and Metallurgical Engineering, University of the Witwatersrand, 2005.
28. Doherty MF, Perkins JD. On the dynamics of distillation processes. I. The simple distillation of multicomponent non-reacting, homogeneous liquid mixtures. *Chem Eng Sci*. 1978;33:281–301.
29. Doherty MF, Perkins JD. On the dynamics of distillation processes. II. The simple distillation of model solutions. *Chem Eng Sci*. 1978;33:569–578.
30. Doherty MF, Perkins JD. On the dynamics of distillation processes. III. The topological structure of ternary residue curve maps. *Chem Eng Sci*. 1979;34:1401–1414.
31. Beneke DA. A novel method for assessing the effect of pressure on vapor–liquid equilibrium in ternary systems. *Ind Eng Chem Res*. 2012;51(11):4371–4379.
32. Holland ST, Tapp M, Hildebrandt D, Glasser D, Hausberger B. Novel separation system design using "Moving Triangles". *Comput Chem Eng*. 2004;29:181–189.
33. Zhang L, Linninger AA. Towards computer-aided separation synthesis. *AIChE J*. 2006;52:1392–1409.
34. Seader JD, Henley EJ. *Separation Process Principles*, 2 ed. Hoboken, N.J.: Wiley, 2006.
35. Engelien HK, Skogestad S. Multi-effect distillation applied to an industrial case study. *Chem Eng Process*. 2005;44:819–826.

Appendix A

This Appendix (Tables A1–A4) gives all physical data used for design for both Aspen Plus® and the CPM method.

$$\ln(P_{VAP}) = C_1 + \frac{C_2}{T + C_3} + C_4 T + C_5 \ln T + C_6 T^{C_7} \quad \text{(A1)}$$

$$C_P^{ig} = C_1 + C_2\left(\frac{C_3/T}{\sinh(C_3/T)}\right)^2 + C_4\left(\frac{C_5/T}{\cosh(C_5/T)}\right)^2 \quad \text{(A2)}$$

Table A1. Binary Interaction Parameters for the Benzene (B), p-Xylene (X) and Toluene (T) System, Used for Both the CPM and Aspen Plus® Designs

	B-X	B-T	X-T
a_{ij}	0	−2.8852	0
a_{ji}	0	2.1911	0
b_{ij}	122.6854	1123.95	75.8978
b_{ji}	−136.481	−863.731	−91.1458
c_{ij}	0.3	0.3	0.3
c_{ji}	0.3	0.3	0.3

Table A2. Coefficients for the Extended Antoine Equation (Eq. 7) Used for Both the CPM and Aspen Plus® Designs (Where P_{VAP} is Measured in kPa and T in °C)

Coefficients	Benzene	p-Xylene	Toluene
C1	76.19924	81.81224	70.03724
C2	−6486.2	−7741.2	−6729.8
C3	0	0	0
C4	0	0	0
C5	−9.2194	−9.8693	−8.179
C6	6.98E-06	6.08E-06	5.30E-06
C7	2	2	2
Lower limit (°C)	5.53	13.26	−94.97
Upper limit (°C)	288.9	343.05	318.6

Table A3. Heat Capacity Coefficients [J/(mol K)] Used for Aspen Plus® Designs Using Eq. 8

Coefficients	Benzene	p-Xylene	Toluene
C1	44.767	75.12	58.14
C2	230.85	339.7	286.3
C3	1479.2	1492.8	1440.6
C4	168.36	224.7	189.8
C5	677.66	675.1	650.43
Lower limit (°C)	−73.15	−73.15	−73.15
Upper limit (°C)	1226.850000	1226.85	1226.85

Table A4. Latent Heat of Vaporixation (kJ/mol) Used for Aspen Plus® Designs

H_{VAP}	Benzene	p-Xylene	Toluene
	30.8036	35.9173	33.3631

Manuscript received May 31, 2012, and revision received Sept. 11, 2012.